Remote Sensing of Environment 179 (2016) 1–12

Contents lists available at ScienceDirect

Remote Sensing of Environment

journal homepage: www.elsevier.com/locate/rse

Seasonal variability of multiple leaf traits captured by leaf spectroscopy at two temperate deciduous forests

Xi Yang [a,b,*], Jianwu Tang [b,**], John F. Mustard [a], Jin Wu [c,e], Kaiguang Zhao [d], Shawn Serbin [e], Jung-Eun Lee [a]

[a] Department of Earth, Environment, and Planetary Sciences, Brown University, Providence, RI 02912, USA
[b] The Ecosystems Center, Marine Biological Laboratory, Woods Hole, MA 02543, USA
[c] Department of Ecology and Evolutionary Biology, University of Arizona, Tucson, AZ 85721, USA
[d] School of Environment and Natural Resources, Ohio Agricultural and Research Development Center, The Ohio State University, Wooster, OH 44691, USA
[e] Environmental & Climate Sciences Department, Brookhaven National Laboratory, Upton, NY 11973, USA

ARTICLE INFO

Article history:
Received 31 August 2015
Received in revised form 16 March 2016
Accepted 23 March 2016
Available online xxxx

Keywords:
Phenology
Leaf physiology
Foliar chemistry
Carbon cycle
Chlorophyll
Carotenoids
Nitrogen
Leaf mass per area
Partial least square regression (PLSR)
Sun and shaded leaves

ABSTRACT

Understanding the temporal patterns of leaf traits is critical in determining the seasonality and magnitude of terrestrial carbon, water, and energy fluxes. However, we lack robust and efficient ways to monitor the temporal dynamics of leaf traits. Here we assessed the potential of leaf spectroscopy to predict and monitor leaf traits across their entire life cycle at different forest sites and light environments (sunlit vs. shaded) using a weekly sampled dataset across the entire growing season at two temperate deciduous forests. The dataset includes field measured leaf-level directional-hemispherical reflectance/transmittance together with seven important leaf traits [total chlorophyll (chlorophyll *a* and *b*), carotenoids, mass-based nitrogen concentration (N_{mass}), mass-based carbon concentration (C_{mass}), and leaf mass per area (LMA)]. All leaf traits varied significantly throughout the growing season, and displayed trait-specific temporal patterns. We used a Partial Least Square Regression (PLSR) modeling approach to estimate leaf traits from spectra, and found that PLSR was able to capture the variability across time, sites, and light environments of all leaf traits investigated (R^2 = 0.6–0.8 for temporal variability; R^2 = 0.3–0.7 for cross-site variability; R^2 = 0.4–0.8 for variability from light environments). We also tested alternative field sampling designs and found that for most leaf traits, biweekly leaf sampling throughout the growing season enabled accurate characterization of the seasonal patterns. Compared with the estimation of foliar pigments, the performance of N_{mass}, C_{mass} and LMA PLSR models improved more significantly with sampling frequency. Our results demonstrate that leaf spectra-trait relationships vary with time, and thus tracking the seasonality of leaf traits requires statistical models calibrated with data sampled throughout the growing season. Our results have broad implications for future research that use vegetation spectra to infer leaf traits at different growing stages.

1. Introduction

Leaf traits are important indicators of plant physiology and critical components in numerous ecological processes (Kattge et al., 2011; Wright et al., 2004). For example, leaf chlorophyll concentration represents the light harvesting potential and is an indicator of photosynthetic activity (Niinemets, 2007; Laisk et al. 2009), while accessory pigments such as carotenoids protect leaves from damage when exposed to excessive sunlight (Demmig-Adams & Adams, 2000). Leaf mass per area (LMA) describes plants' investment to leaves in terms of carbon and nutrients to optimize sunlight interception (Poorter, Niinemets, Poorter, Wright, & Villar, 2009). Carbon is one of the major elements in cellulose and lignin, which are used to build the cell walls of various leaf tissues (Kokaly, Asner, Ollinger, Martin, & Wessman, 2009). Nitrogen is the key element in both carbon fixation enzyme RuBisCO and chlorophyll (Evans, 1989a, 1989b), and thus plays an important role in modeling leaf and canopy photosynthesis (Bonan, Oleson, Fisher, Lasslop, & Reichstein, 2012). The aforementioned leaf traits, as well as the corresponding spectral properties, strongly depend on leaf developmental stages and light environments (Yang, Tang, & Mustard, 2014; Lewandowska & Jarvis, 1977; Poorter et al., 2009; Wilson, Baldocchi, & Hanson, 2000; Wu et al., 2016a). Thus, capturing the spatial and temporal variations of these leaf traits is important for understanding terrestrial ecosystem functioning (Schimel et al., 2015).

Despite the importance and increasing interests in the temporal and spatial variability of these (and many other) leaf traits, the capacity to monitor these traits over seasons has not progressed accordingly. Wet

* Correspondence to: X. Yang, Department of Earth, Environment, and Planetary Sciences, Brown University, Providence, RI 02912, USA.
** Corresponding author.
E-mail addresses: xi_yang@brown.edu (X. Yang), jtang@mbl.edu (J. Tang).

http://dx.doi.org/10.1016/j.rse.2016.03.026
0034-4257/

chemical analysis of these leaf traits is considered to be the standard method, yet the destructive and time-consuming protocols do not allow for rapid and repeated sampling of some traits. On the other hand, field spectroscopy can augment traditional approaches, and allows for repeated sampling of the same leaves and thus tracking time-sensitive changes such as frost damage (Asner & Martin, 2008; Couture, Serbin, & Townsend, 2013; Serbin, Singh, McNeil, Kingdon, & Townsend, 2014). Although spectroscopic approaches are promising, many previous efforts have only focused on mature sunlit leaves (e.g., Asner & Vitousek, 2005; Ustin, Roberts, Gamon, Asner, & Green, 2004; Wicklein et al., 2012; but see Sims and Gamon (2002)) and have not explored the ability of leaf spectral properties to track the continuous and developmental changes of leaf traits throughout the growing season. The temporal dimension of the spectra-trait relationship has mostly focused on leaf chlorophyll concentration (Belanger, Miller, & Boyer, 1995; Dillen, de Beeck, Hufkens, Buonanduci, & Phillips, 2012; Shen, Chen, Zhu, & Tang, 2009; Zhang et al., 2007), while it is largely unknown for other important leaf traits like nitrogen, carbon, and LMA. Moreover, the availability of high temporal resolution (~weekly) datasets on important leaf traits and spectra is limited. These data would be very useful for assessing the utility of leaf spectral properties (i.e. reflectance) for estimating the temporal variability of leaf traits, as well as scaling to broader regions and informing process modeling activities.

Leaf traits not only change with time, but also with the light environments, such as moving from sun-lit to shaded light conditions and the commensurate changes in microclimate which also affect leaf traits (Ellsworth & Reich, 1993; Niinemets, 2007; Wu et al., 2016b), as a consequence of underlying fundamental evolutionary and ecophysiological constraints (Terashima, Miyazawa, & Hanba, 2001). For example, shaded leaves display lower chlorophyll *a* to *b* ratio and higher LMA compared with sunlit leaves (Niinemets, 2007). This variation in the vertical domain can be as much as the trait variation across space (Serbin et al., 2014). As such, it is important to not only explore trait variation across sites but also as in the vertical canopy light gradients to better capture ecosystem responses to global change.

Three categories of methods to estimate leaf traits from leaf spectral properties (i.e., reflectance and transmittance) are spectral vegetation indices (SVIs), statistical inversion methods exploiting the full wavelength (400–2500 nm), and leaf radiative transfer models like PROSPECT (Jacquemoud & Baret, 1990), which are limited to only a few leaf traits (do not include carbon and nitrogen) and thus are not the focus of this study. SVIs are typically calculated using the reflectance from two or three wavelengths (Huete et al., 2002; Richardson, Duigan, & Berlyn, 2002; Sims & Gamon, 2002). With proper calibration across a diverse range of vegetation types, SVIs can yield relatively robust models (Féret et al., 2011). Statistical methods such as Partial Least Square Regression (PLSR) modeling have become more popular in recent decades with the availability of high spectral resolution observations and increasing computational power (Asner & Martin, 2008; Couture et al., 2013; Wold, Sjöström, & Eriksson, 2001). Although both being widely used, these methods have not been thoroughly assessed, especially with respect to the robustness of PLSR models across time and different light environments (but see Serbin et al., 2014).

Here our primary goal was to assess the ability of leaf optical properties to track temporal variability of a suite of leaf traits across sites and different light environments. To explore this we collected a dataset of ~weekly-sampled leaf traits [including total chlorophyll (and chlorophyll *a* and *b*), carotenoids, mass-based nitrogen concentration (N_{mass}), mass-based carbon concentration (C_{mass}), and LMA] along with in situ directional-hemispherical reflectance/transmittance during the growing season at two temperate deciduous forests. We first present the temporal variations of leaf traits and spectra, and then highlight the ability of leaf spectra to track temporal variability of leaf traits. We investigate the robustness of the PLSR across season, sites, and light environments. We further explore the optimal field sampling strategy. We conclude by discussing the broad implications of our study.

2. Study area and methods

2.1. Study sites

Our field sampling was conducted in two temperate deciduous forests located in the northeastern United States. The first site, on the island of Martha's Vineyard (MV, 41.362N, 70.578W), is a white oak (*Quecus alba*) dominated forest with a stand age of 80–115 years after natural recovery from abandoned cropland and pasture (Foster, Hall, Barry, Clayden, & Parshall, 2002). Mean annual temperature is 10 °C, and annual precipitation is about 1200 mm from 1981 to 2010 (Yang et al., 2014). The second site, in Harvard Forest (HF, 42.538N, 72.171W), has two dominating deciduous tree species: red oak (*Quercus rubra*) and red maple (*Acer rubrum*), with a few scattered yellow birch (*Betula alleghaniensis*). The forest age is 70–100 years. The annual mean temperature is about 7.5 °C (Wofsy et al., 1993), and the annual precipitation is 1200 mm. Remote sensing studies suggested that the start of season in Martha's Vineyard was about 10–20 days later than that of HF (Fisher & Mustard, 2007; Yang, Mustard, Tang, & Xu, 2012).

2.2. Measurements of leaf spectral properties and traits

We conducted two field campaigns to collect leaf traits at the sites in Martha's Vineyard and Harvard Forest, respectively. In 2011, weekly (biweekly in August) sampling of leaves throughout the growing season (June–November) was conducted at the Martha's Vineyard site on three white oak trees. For each sampling period, we cut two fully sunlit branches (each having ~6 leaves) and one shaded branch using a tree pruner. The spectral properties of the leaves were immediately measured (see below). Then the leaves were placed in a plastic bag containing a moist paper towel, and all the samples were kept in a cooler filled with ice until being transferred back to the lab for further measurements. In 2012, the same weekly (biweekly from mid-July to late August) measurements in Harvard Forest were made on five individuals (two red oaks, two red maples and one yellow birch) from May to October. For each tree, two sunlit and one shaded branch were collected each time.

Directional-hemispherical leaf reflectance and transmittance were measured immediately after the sampling using a spectroradiometer (ASD FS-3, ASD Inc. Boulder, CO, USA; spectral range: 300–2500 nm, spectral resolution: 3 nm@700 nm, 10 nm@1400/2100 nm) and an integrating sphere (ASD Inc.). The intensity of light source in the integrating sphere decreases sharply beyond 2200 nm, with the signal in 2200–2500 nm being noisy (ASD Inc., personal communications), and thus is excluded from the spectral-leaf traits analysis below.

The measured leaf traits include total chlorophyll concentration (including chlorophyll *a* and chlorophyll *b*, μg/cm^2), carotenoids (μg/cm^2), leaf mass per area (LMA, g/m^2), nitrogen concentration by mass (N_{mass}, %), and carbon concentration by mass (C_{mass}, %). Each branch was divided into two subsets. One subset was used to measure pigment concentrations. To measure the chlorophyll *a*nd carotenoids concentration, three leaf discs (~0.28 cm^2 each) were taken from each leaf using a hole puncher, and then ground in a mortar with 100% acetone solution and MgO (Asner, Martin, Ford, Metcalfe, & Liddell, 2009). After an 8-minute centrifugation, the absorbance of the supernatant was measured using a spectrophotometer (Shimadzu UV-1201, Kyoto, Japan). Chlorophyll *a*, *b* and carotenoids concentrations were calculated using the readings from 470, 520, 645, 662 and 710 nm (Lichtenthaler & Buschmann, 2001). The other subset (3 leaves) was scanned using a digital scanner (EPSON V300, EPSON, Long Beach, CA, USA), and oven-dried (65 °C) for at least 48 h for quantification of leaf dry mass. LMA was calculated based on the following equations:

$$LMA = W_{dry}/A_{leaf}$$

Table 1
Simple vegetation indices (SVI) used in this study. These indices were calibrated using extensive datasets (Féret et al., 2011). Leaf traits were calculated based on a polynomial relationship: leaf trait = a × index^2 + b × index + c.

Leaf traits	Index	Coefficients		
		a	b	c
Chl (μg/cm^2)	$(R_{780} - R_{712})/(R_{780} + R_{712})$	40.65	121.88	−0.77
Car (μg/cm^2)	$(R_{800} - R_{530})/(R_{800} + R_{530})$	8.09	11.18	−0.38
LMA (g/cm^2)	$(R_{1368} - R_{1722})/(R_{1368} + R_{1722})$	−0.1004	0.1286	−0.0044

where W_{dry} is leaf dry mass weight, A_{leaf} is the leaf area calculated from the scanned leaf using ImageJ (Schneider, Rasband, & Eliceiri, 2012). Dried leaves were then ground and analyzed for N_{mass} and C_{mass} with a CHNS/O analyzer (FLASH 2000, Thermo Scientific, Waltham, MA, USA).

2.3. Methods to estimate leaf traits using leaf spectral properties

We used two categories of methods to estimate leaf traits based on leaf spectral properties: vegetation indices that utilize the reflectance from two wavelengths, and statistical methods that exploit the information from the full leaf spectrum.

Based on extensive datasets from various types of biomes and plants, Féret et al. (2011) established polynomial relationships between SVIs and total chlorophyll concentration, carotenoids and LMA (Table 1). We also obtained the best estimate of a, b, and c using our own dataset (see below for the division between training and validation dataset).

The second category of methods essentially is to build multivariate linear regression models between leaf spectra and leaf traits (Zhao, Valle, Popescu, Zhang, & Mallick, 2013):

$$\mathbf{y} = \mathbf{X} \cdot \beta + \varepsilon$$

where **y** is an n-by-1 matrix of leaf traits (n equals to the number of leaf samples). **X** is an n-by-m matrix (m equals the number of bands from each spectrum, and thus in this study m = 1801: from 400 to 2200 nm). ε is the n-by-1 estimation error that is to be minimized. PLSR modeling can be used to develop the best model for the given dataset while avoid over-fitting (Asner & Martin, 2008; Serbin et al., 2014). The numbers of independent factors used in the regression were determined by minimizing the Prediction Residual Error Sum of Squares (PRESS).

The above leaf traits and spectra from two sites were combined as one single dataset. To test the effectiveness of PLSR on this dataset, the whole dataset is divided into two parts (70%–30%), for the training and validation of PLSR, respectively. We used the Kennard-Stone algorithm to select the training subset that provides a uniform coverage of the whole dataset (Kennard & Stone, 1969). The training dataset was used to optimize the regression model parameters (β), and then the validation dataset was used to test and evaluate the PLSR models. Evaluation statistics include the R^2, Root Mean Square Error (RMSE) and normalized RMSE (NRMSE), which is the RMSE divided by the range of the estimated leaf traits.

The relative importance of reflectance or transmittance at each wavelength is determined by calculating the values of variable importance on projection (VIP) (Wold et al., 2001). VIP is an indicator of the importance of each wavelength for the modeling of both leaf traits (**y**) and spectra (**X**). Higher absolute values indicate greater importance of the corresponding wavelength. Generally, wavelengths with VIP value larger than 1 are considered being important (Mehmood, Liland, Snipen, & Sæbø, 2012).

2.4. Robustness of PLSR models and scenarios for field sampling design

To examine the robustness of PLSR models across time, light environment, and sites, we designed the following scenarios. In all scenarios, we used leaf traits and spectra of a subset of the whole dataset (e.g., leaf samples that are collected during only a certain period of time, or a certain level of light environment) to train PLSR models, and tested the performance of the models against the whole dataset.

For this we created five scenarios to examine how the timing of leaf sampling affects predictability of seasonality of leaf traits. Leaf traits and spectra in the first three scenarios were sampled only for the spring, summer, and fall, respectively. We defined these three seasons based on variations in total chlorophyll concentration: days before total chlorophyll reached a plateau in the mid-season were defined as spring; days when total chlorophyll started to decrease were defined as fall; and between spring and fall, days were defined as summer. The last two scenarios were that leaf traits and spectra were sampled monthly or biweekly (instead of weekly as in the full dataset). We then use the PLSR trained with leaf samples in the above scenarios to predict the leaf traits of the entire dataset. There are two reasons to choose the whole dataset for validation: 1) the whole dataset captures the temporal variability of leaf traits, which is the goal of this test and 2) it is necessary to have the same validation dataset to compare the performance of these five scenarios. Performance of these sampling strategies was measured by calculating the RMSE and R^2.

Finally, we also explored our capacity to develop a generalized approach for capturing seasonality in leaf traits with spectral observations. Two tests were conducted to examine the robustness of PLSR models at different light environment and sites. Test 1 used sunlit leaf traits and spectra to train a PLSR model, which was then used to predict shaded leaf traits with corresponding spectra. We then switched the training and validation datasets so that shaded leaves were used to train PLSR model while sunlit leaves were used to validate. Test 2 divided the entire dataset into two subsets by geographic location. For example, we used Martha's Vineyard dataset to calibrate the model, and Harvard Forest dataset to validate, and vice versa.

3. Results

3.1. Temporal and spatial variability of leaf traits

All leaf traits displayed significant temporal variations throughout the growing seasons (Figs.1 and 2). Overall, pigments from both sites displayed similar bell-shaped trajectories, despite being sampled from different species and locations within the canopy. Chlorophyll concentration rapidly increased from ~10 μg/cm^2 at the beginning of the season, and then stabilized around ~50 μg/cm^2 and ~40 μg/cm^2 in Martha's Vineyard and Harvard Forest, respectively, during the summer followed by a decline in the fall to values similar to the beginning of the season prior to leaf abscission. The Harvard Forest samples were collected from three different species, and showed much larger variability compared with Martha's Vineyard, especially for the shaded leaves (Fig.1e–h). The carotenoids concentration was ~3 μg/cm^2 at the beginning/end of the season and ~10 μg/cm^2 at the peak season. The total chlorophyll concentration relative to the carotenoids concentration (Chl/Car) increased during the early seasons. In the fall, though both chlorophyll and carotenoids decreased, Chl/Car decreased steadily, as a result of faster decline of chlorophyll relative to the carotenoids (Fig. S1a).

The remaining three leaf traits (LMA, N_{mass}, and C_{mass}) displayed different seasonal patterns compared with leaf pigments (Fig. 2). For example, LMA rapidly increased in the spring, but showed only a minor decline by the end of the measurement period. N_{mass} was higher (~4–5%) at the start of the season, and remained stable around 2% during the summer, followed by ~1% decrease in the fall, presumably caused by nitrogen resorption (Eckstein, Karlsson, & Weih, 1999). Similar to

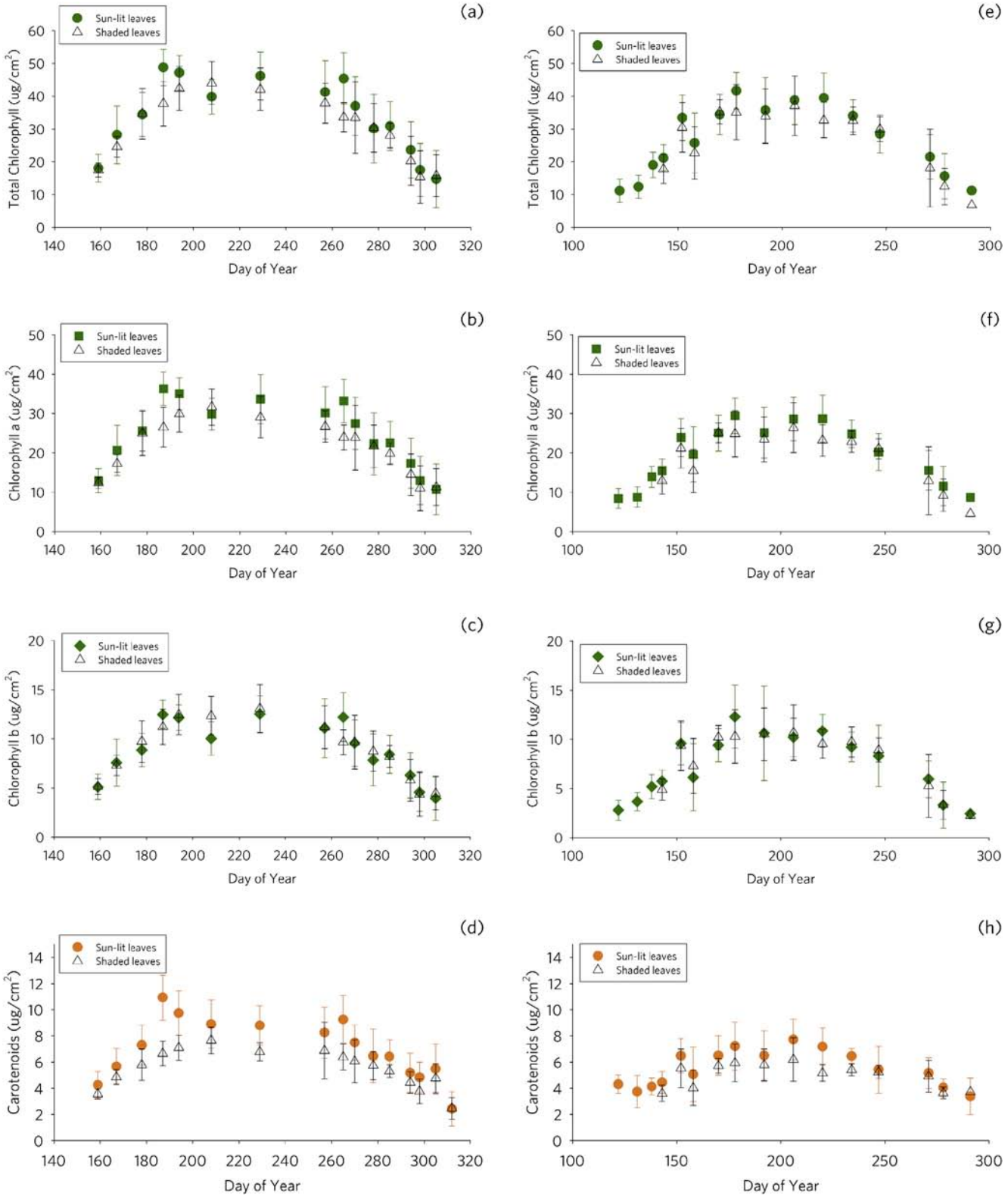

Fig. 1. Seasonal patterns of pigments of sunlit (filled) and shaded (open) leaves from two deciduous forests. Martha's Vineyard, year 2011: (a) Total chlorophyll; (b) chlorophyll *a*; (c) chlorophyll *b*; (d) carotenoids. Harvard Forest year 2012: (e) Total chlorophyll; (f) chlorophyll *a*; (g) chlorophyll *b*; (h) carotenoids. Each dot is the mean value of all the samples collected that day. Error bars are standard deviations.

LMA, C_{mass} accumulated 2–4% in the spring and stabilized for the rest of the growing seasons around 50%. The rapid increase of LMA in the spring was accompanied by a similar increase of C_{mass} and decrease of N_{mass}, which all ended at the same time (DOY ~194 in Martha's Vineyard, and DOY ~170 in Harvard Forest).

Mean annual values of leaf traits from Martha's Vineyard were significantly different from those at Harvard Forest (Table 2). For example, leaf chlorophyll in Martha's Vineyard is 5.64 μg/cm^2 (17.5%) higher than that from Harvard Forest ($p < 0.0001$). LMA in Martha's Vineyard showed much larger variation than that from Harvard Forest, and the

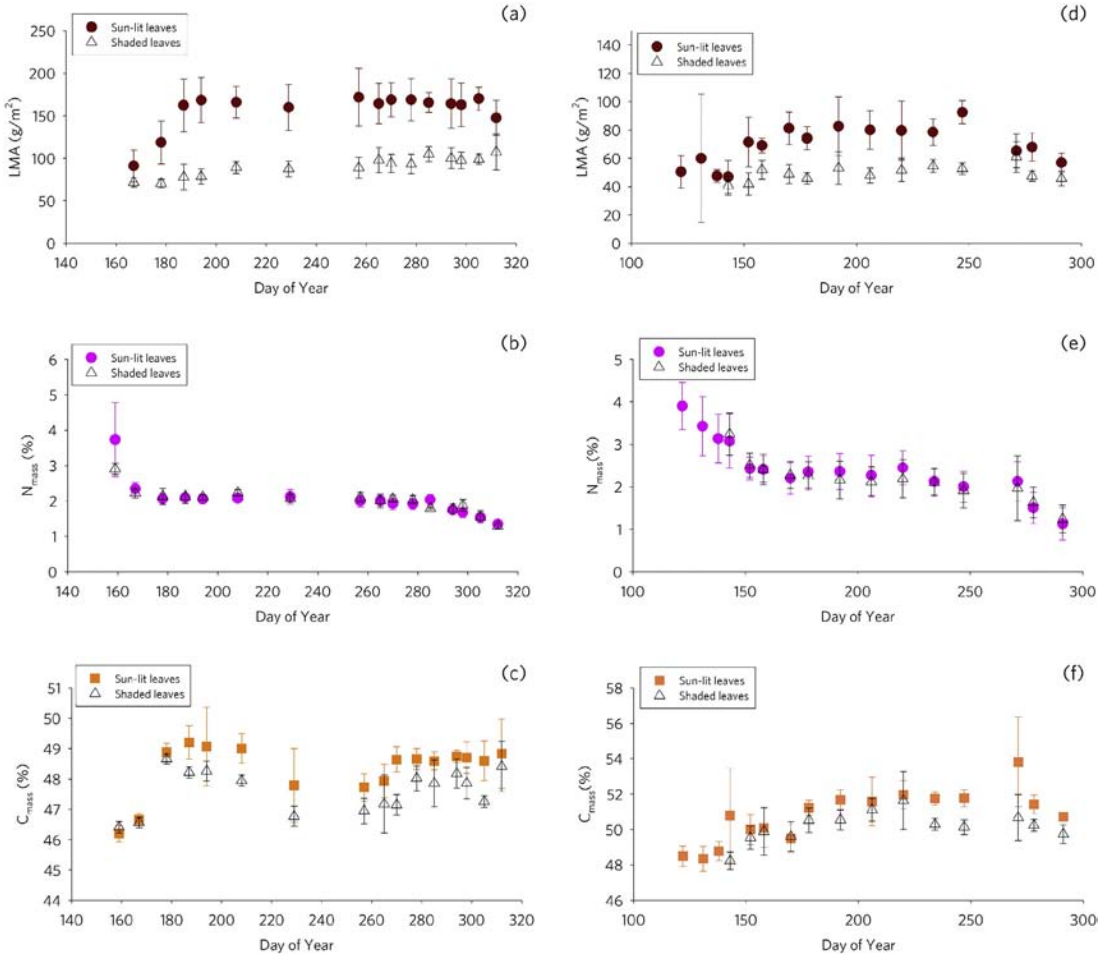

Fig. 2. Seasonal patterns of biochemical and biophysical properties of sunlit (filled symbols) and shaded (open symbols) leaves from two deciduous forest sites. Martha's Vineyard, year 2011: (a) Leaf mass per area (LMA); (b) mass-based nitrogen concentration (N_{mass}); (c) mass-based carbon concentration (C_{mass}). Harvard Forest, year 2012: (d) LMA; (e) N_{mass}; (f) C_{mass}. Each dot is the mean value of all the samples collected that day. Error bars are standard deviations.

mean LMA was 39.85 g/m^2 (37.5%) higher than that from Harvard Forest. Similar situation applies to all other leaf traits except for C_{mass}, for which the value at Harvard Forest were higher than that at Martha's Vineyard.

Sunlit leaves contained more total chlorophyll and carotenoids (Fig. S2) and the carotenoids to the total chlorophyll ratio was significantly higher for sun-lit leaves comparing with shaded leaves (MV, $p < 0.0001$; HF, $p = 0.0182$). Chlorophyll *a*/*b* was also significantly larger for sunlit leaves in both sites (MV, $p < 0.0001$; HF, $p < 0.0001$). Similarly, LMA and C_{mass} values were significantly higher in the sun-lit leaves versus shaded foliage, with the only exception of N_{mass}, in which both sun-lit and shaded leaves were indistinguishable throughout the two seasons (Fig. 2b).

A linear regression analysis highlighted various levels of correlation among leaf traits (Fig. 3). Close correlation was found among leaf pigments: total chlorophyll concentration was highly correlated with carotenoids concentration ($R^2 = 0.85$), suggesting a tight coupling among those pigments throughout the growing season despite the faster decrease of chlorophyll concentration during the senescence (Fig. S1). For the entire dataset (across all sunlit and shaded leaves from different species), N_{mass} was weakly correlated with pigments. LMA showed positive correlation with all pigments while a negative correlation was observed with N_{mass} and C_{mass}.

Table 2
Annual mean values and standard deviation of leaf traits at two sites: MV, Martha's Vineyard, and HF, Harvard Forest (stars indicate the *p*-values of *t*-test between the values of leaf traits from two sites).

Leaf traits	Units	MV	HF
Total Chl***	μg/cm^2	31.74 (12.17)	26.19 (9.29)
Chl *a***	μg/cm^2	23.19 (8.81)	18.92 (6.70)
Chl *b***	μg/cm^2	8.70 (3.31)	7.48 (2.73)
Car**	μg/cm^2	6.16 (2.28)	5.59 (1.33)
N_{mass}**	% (unitless)	2.17 (0.50)	2.03 (0.50)
C_{mass}***	% (unitless)	48.34 (1.24)	51.12 (0.87)
LMA***	g/m^2	106.29 (45.04)	66.44 (15.56)

*** $p < 0.0001$.
** $p < 0.01$.

3.2. Seasonal variability of leaf spectral properties

The full leaf reflectance and transmittance spectrum showed significant variability in both amplitude and shape (Fig.4). The visible (VIS, 400–700 nm) and near infrared (NIR, 700–1000 nm) changed dramatically throughout the season, while shortwave infrared (SWIR 1000–2500 nm) was relatively stable. Data from Martha's Vineyard showed larger variability in NIR compared to Harvard Forest.

The R, G, and B reflectance at both sites showed a U-shape pattern (Fig. S3a, S3c): all of them decreased in the beginning of the season; and increased in the end of the season after a stable summer. The NIR from Martha's Vineyard showed a consistent decline in the mid-

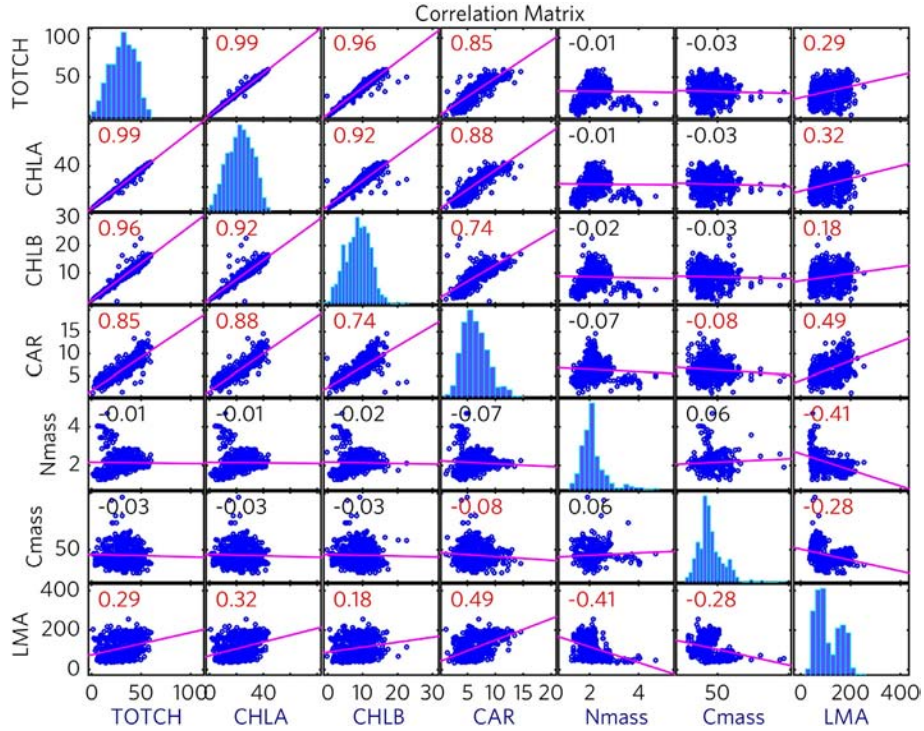

Fig. 3. Correlation matrix of all the leaf traits. Histograms of each leaf traits are on the diagonal positions. Number on each subplot indicates R^2 (Red means $p < 0.05$). See Table 2 for units.

summer and then increased in the fall, while the NIR from Harvard Forest was relatively stable throughout the season. Leaf transmittance at each band had similar patterns as the reflectance (Fig. S3b, S3d).

3.3. Comparisons of methods of leaf traits estimation

We compared two categories of methods to estimate leaf traits from leaf spectra. Overall, PLSR consistently outperformed the SVIs in estimating leaf traits, showing an improved performance when the SVIs were trained by the original datasets or our own dataset (Table 3). The PLSR models using leaf reflectance ($PLSR_{ref}$ hereafter) had slightly better performance compared with those using leaf transmittance ($PLSR_{tra}$ hereafter) when assessed with the independent dataset. For different leaf traits, the performance of these methods varied, as described in details below.

Leaf chlorophyll from the validation dataset was well estimated by $PLSR_{ref}$ (Fig.5. $R^2 > 0.70$ and NRMSE < 10%). The SVI for chlorophyll showed slightly larger prediction error (~0.5 μg/cm^2 larger) compared

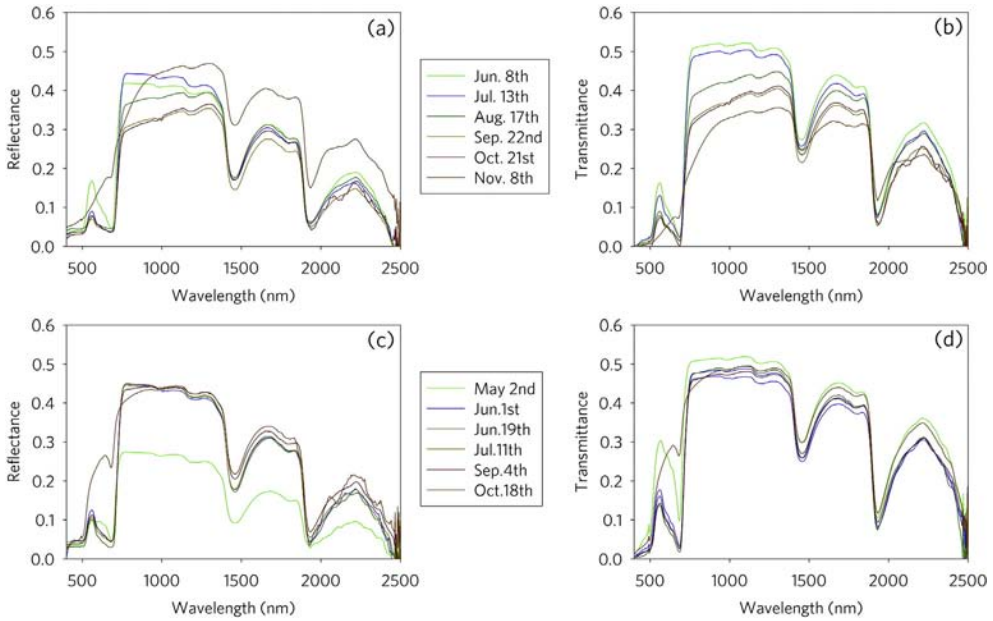

Fig. 4. Examples of leaf directional-hemispherical reflectance and transmittance measured on (a, b) Martha's Vineyard and in (c, d) Harvard Forest.

Table 3
Comparisons among methods in terms of the goodness-of-fit (RMSE, NRMSE and R^2) for the dataset at both Martha's Vineyard and Harvard Forest. $PLSR_{ref}$ indicates models using reflectance dataset to predict leaf traits. $PLSR_{tra}$ indicates models using transmittance dataset to predict leaf traits.

Leaf traits	RMSE (NRMSE)				R^2			
	Simple indices (Féret et al., 2011)	Simple indices (this dataset)	$PLSR_{ref}$	$PLSR_{tra}$	Simple indices (Féret et al., 2011)	Simple indices (this dataset)	$PLSR_{ref}$	$PLSR_{tra}$
Total Chl (μg/cm^2)	5.93	6.04	5.48 (0.09)	5.62 (0.10)	0.71	0.71	0.73	0.64
Chl *a* (μg/cm^2)			3.99 (0.09)	4.14 (0.09)			0.73	0.68
Chl *b* (μg/cm^2)			1.62 (0.07)	1.82 (0.08)			0.66	0.58
Car (μg/cm^2)	1.53	1.54	1.07 (0.08)	1.20 (0.09)	0.39	0.40	0.71	0.68
N_{mass} (%)			0.22 (0.05)	0.24 (0.05)			0.63	0.54
C_{mass} (%)			0.93 (0.07)	0.95 (0.07)			0.63	0.71
LMA (g/cm^2)	40.6	39.7	18.11 (0.08)	19.01 (0.09)	0.20	0.19	0.85	0.79

with $PLSR_{ref}$ and $PLSR_{tra}$ (Table 3). The two components of chlorophyll (Chl *a* and *b*) were also well captured by the $PLSR_{ref}$ approach with NRMSE < 10% and R^2 of 0.73 and 0.66 respectively. Similarly, carotenoids were estimated relatively well by $PLSR_{ref}$ and $PLSR_{tra}$ ($R^2 > 0.65$) but the SVI for carotenoids had 30% higher RMSE comparing with $PLSR_{ref}$.

N_{mass} was well captured by leaf spectra especially with the reflectance dataset (Fig.5. $R^2 > 0.6$ and NRMSE < 5%). Similarly, both $PLSR_{ref}$ and $PLSR_{tra}$ explained ~60% of the variance in C_{mass} ($R^2 > 0.6$ and NRMSE < 7%). PLSR also displayed a strong capacity to predict LMA ($R^2 = \sim 0.80$ and NRMSE < 9%), where the SVI for LMA could not capture >20% of the variation in LMA and had more than double the RMSE of $PLSR_{ref}$ mainly due to a saturation effect (data not shown).

The VIP values of PLSR show the relative importance of each wavelength in predicting leaf traits (Fig.6). Visible and near-infrared wavelengths were important to the prediction of leaf pigments; there are three peaks (400, 550 and 730 nm) that are related to the chlorophyll absorption in the red (620–750 nm) and blue (400–450 nm), and reflection in the green (495–570 nm). The two components of chlorophyll (*a* and *b*) were also mainly contributing to the red/NIR region (600–750 nm), and the main contributing bands for chl *b* shifted towards green comparing to those for chl *a* (Fig. 6b and 6c) (Ustin et al., 2009). Carotenoids have a similar VIP curve comparing with the chlorophyll, with one distinction: the VIP values for carotenoids between 650 nm and 700 nm are relatively higher to those of chlorophyll.

Compared with the pigments, N_{mass}, C_{mass} and LMA have relatively smooth VIP curves. For N_{mass}, wavelengths around 700 nm and beyond 1900 nm are important to the prediction of N_{mass}, presumably because the visible region is controlled by pigments and nitrogen is an important component in leaf pigments, and the SWIR region near 2000 nm is controlled by protein absorption features (Kokaly et al., 2009). Both C_{mass} and LMA were related to the leaf structure and were largely contributing to the reflectance at NIR and SWIR.

3.4. Robustness of the PLSR approach across time, sites and light environment

We examined the performance of the $PLSR_{ref}$ models under five scenarios where different sampling strategies were applied. The performance of the PLSR models generally improved in the order of spring, fall, summer, monthly, and biweekly (Table 4). As expected, more sampling throughout the season (and the increasing size and representativeness of the calibration dataset) increased R^2 and reduced RMSE. When comparing the three seasons, summer-only sampling yielded higher model performance relative to the other two scenarios, yet the improvements from scenarios 2 (summer-only) to scenario 4 (monthly) were not as obvious for pigments as N_{mass}, C_{mass} and LMA. Sampling scenario 5 (biweekly) largely improved the performance of PLSR, especially for N_{mass} and C_{mass} (R^2 increased from <0.4 to ~0.6).

Examining the seasonal patterns of predicted and observed leaf traits revealed time-dependent performance of each scenario. In spring-only scenario where leaf samples only from the spring were used for PLSR calibration, all leaf traits during the first four weeks of the growing seasons were well estimated. However, fall season leaf traits were overestimated except for LMA in Martha's Vineyard (Fig. S4m). By contrast, in the fall-only scenario, spring and summer leaf traits were underestimated except for C_{mass} (Fig. S5k). Summer-only scenario showed a better ability to capture the seasonal patterns of leaf traits, only underestimated the N_{mass} peak in the early spring at Harvard Forest (Fig. S6j). The monthly sampling scenario improved estimation of all leaf traits, in which the improvement on estimating LMA was the most obvious (R^2 from 0.26 in the summer case to 0.76 in the monthly sampling case, Fig. S7m, S7n). Biweekly sampling scenario appeared to produce a satisfactory result for all the leaf traits studied here (Fig. S8).

$PLSR_{ref}$ models trained using sunlit leaves explain 35%–70% of the variability in shaded leaves with highest R^2 for pigments while lowest R^2 for C_{mass} (Fig. S9, Table S1). However, $PLSR_{ref}$ was less accurate for leaf traits like LMA in terms of RMSE (Fig. S10 m), for which the difference between sun-lit and shaded leaves was significant (Fig. 2). Similarly, $PLSR_{ref}$ models trained with shaded leaves were able to predict the sunlit leaf traits, but with lower model performance compared to when trained with sunlit foliage. Depending on the leaf traits, the variability explained by PLSR ranges from 35% to 70% (Fig. S10m).

$PLSR_{ref}$ models trained using data from Harvard Forest (Test 1) were able to capture 60–70% of variability of the pigments from Martha's Vineyard, except for N_{mass} and C_{mass} (Table 5). Similar results were obtained from $PLSR_{ref}$ trained using Martha's Vineyard data (Test 2) and validated with Harvard Forest data. VIP values for pigments in Test 1 were similar to those from Test 2. This is in stark contrast with VIP values for Nmass, Cmass, and LMA from both experiments. The locations of important wavelengths were quite different between two tests (Fig. S11).

4. Discussion

4.1. Can we track the seasonality of leaf traits using leaf spectroscopy?

Here we show that the seasonal variability of leaf traits can be well captured with leaf spectroscopy approaches (Fig.5, Table 3). All leaf properties (seven leaf traits and leaf spectra) display seasonal dynamics that are also related to the location and microclimate (i.e., sunlit vs. shaded, and the accompanying changes in humidity and temperature). The PLSR models explain 60%–80% of variability of these leaf traits in our study, supporting the hypothesis that leaf spectra can capture the seasonal variability of leaf traits. Indeed, each leaf trait has its own spectral fingerprint (Curran, 1989; Kokaly et al., 2009), as we have seen from the VIP values of PLSR models (Fig.6). Patterns of VIP values were similar to previous studies (Asner et al., 2009; Serbin et al., 2014) and consistent with our understandings of leaf physiology (Ustin et al., 2009). This is an important result as collecting leaf spectra is much more time-efficient than traditional approaches and allows for repeated sampling of the same leaves throughout the season. SVIs can be an alternative

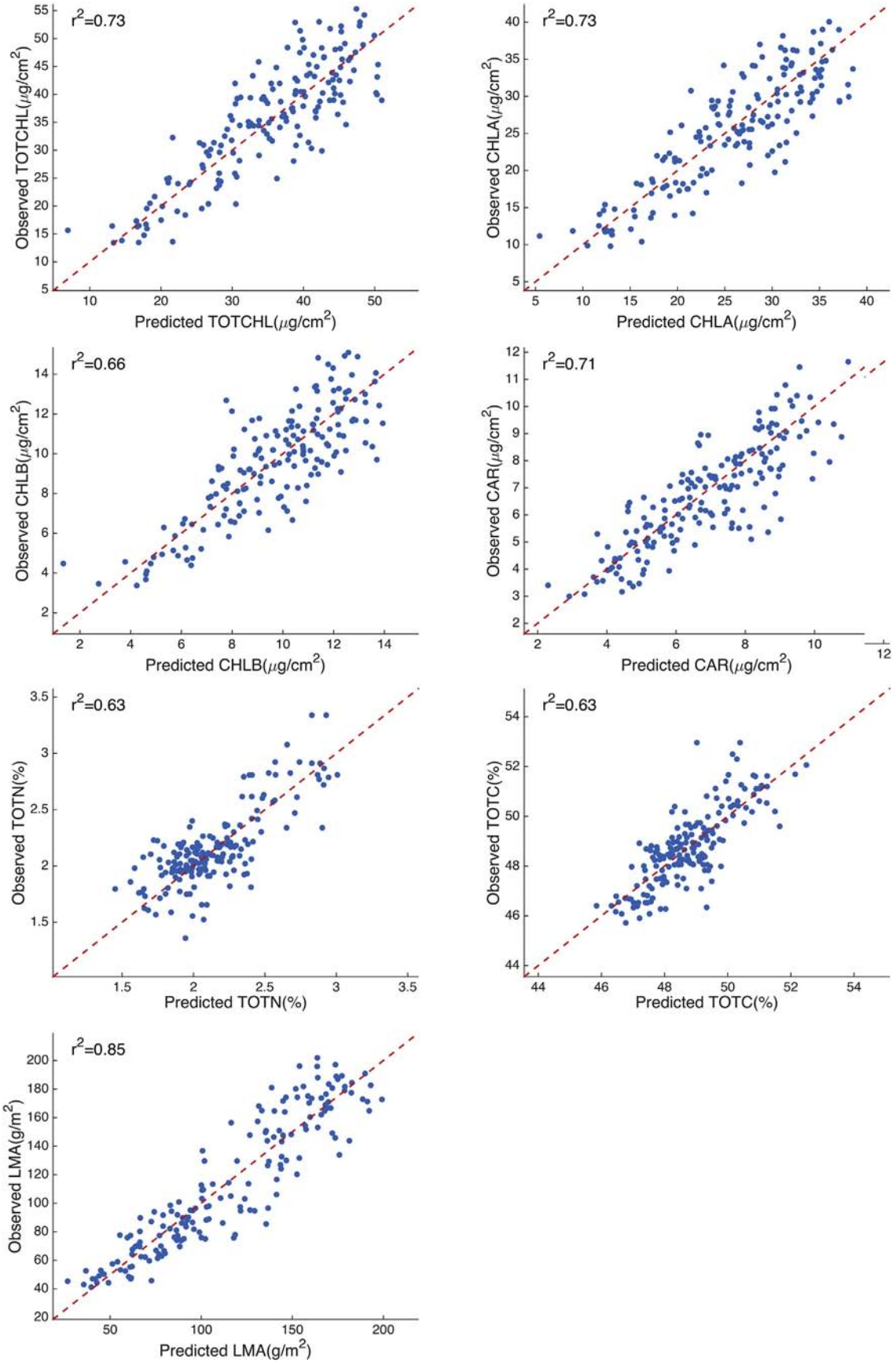

Fig. 5. Comparisons between the observed leaf traits and predicted traits from $PLSR_{ref}$. For detailed statistics, refer to Tables 2 and 3. Observations are from the independent validation dataset selected using the Kennard-Stone method. The red dashed lines are 1:1 line.

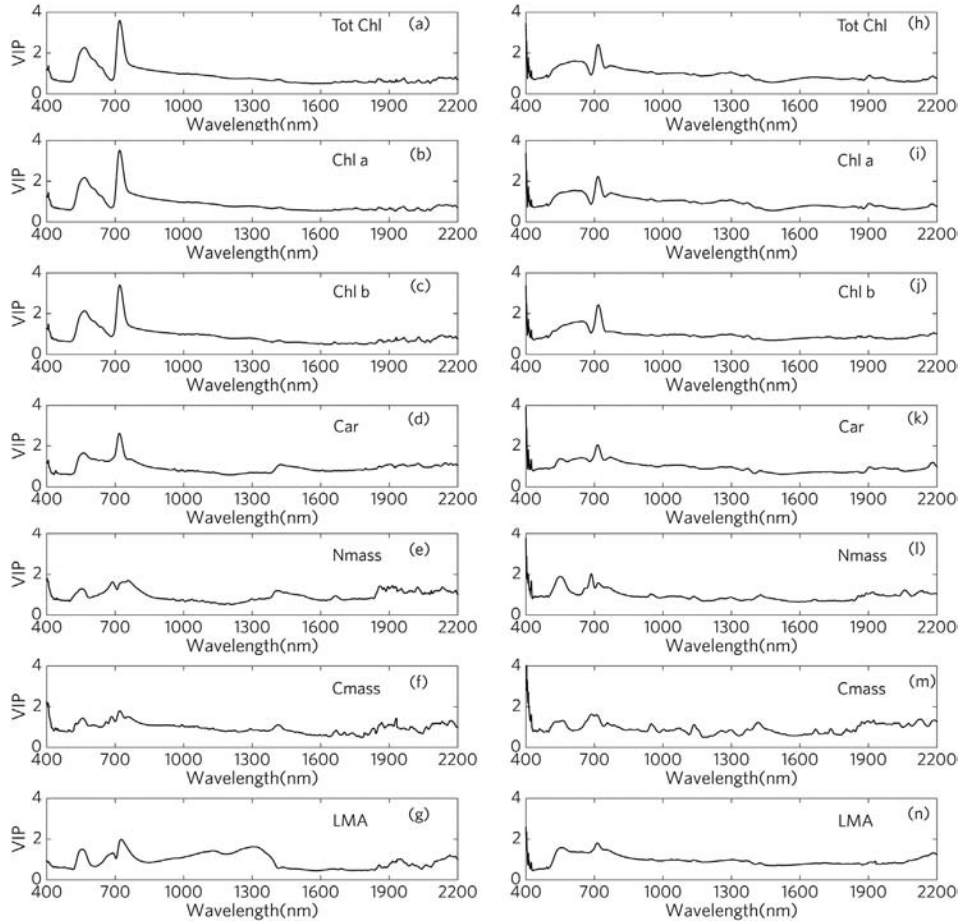

Fig. 6. Relative importance of each wavelength in variable importance on projection (VIP). VIP values from $PLSR_{ref}$ and $PLSR_{tra}$ are on the right and left, respectively.

for the estimation of total chlorophyll concentration when there are limits on available instruments or, for example, using two-band LED sensors (e.g. Garrity, Vierling, & Bickford, 2010; Ryu et al., 2010). The result also has implications for the current and future use of field spectrometers that measure leaf or canopy reflectance at high temporal frequency (e.g., Hilker et al., 2009). Our well-calibrated PLSR models can be used on leaf reflectance to track the seasonality of multiple leaf traits in temperate deciduous forests.

The tests on the robustness of leaf spectra-trait relationships suggested that the overlap between the training dataset and an independent validation dataset is important for a good prediction. Traditionally, the development of the leaf traits-spectra relationship has been focused on a single time point, typically mid-season and mature leaves. Summer mature leaves displayed higher pigments concentration and LMA, while lower N_{mass} compared with young leaves (Fig. 1, Fig. 2). In addition, the corresponding leaf spectra were significantly different (Fig. 4). We have shown here that if we apply an empirical relationship between spectra and traits derived from one period (for example, summer) to another (spring or fall), leaf traits will likely be over or under-estimated (Fig. S4–S6). These findings mirror that observed by McKown, Guy, Azam, Drewes, and Quamme, 2013 which used traditional trait measurements across key phenophases of a temperate forest species, *Populus trichocarpa*, to show that the direction and magnitude of many trait-trait relationships is strongly tied to phenological state and can change over a season. However, we have also illustrated that with proper calibration, we can adequately characterize the seasonality of a range of leaf traits, despite the impacts of phenology, which is critical for monitoring ecosystems and informing large-scale modeling activities (Table 5).

VIP values can help to explain the prediction power of PLSR models. For example, in the case of PLSR models trained with data from one site to predict another (Tests 1 & 2), VIP values of leaf pigments overlap

Table 4
Performance of all scenarios (spring, summer, fall, monthly, and biweekly) in terms of the goodness-of-fit (RMSE, R^2).

Leaf traits	RMSE					R^2				
	Spring	Summer	Fall	Monthly	Biweekly	Spring	Summer	Fall	Monthly	Biweekly
Total Chl (μg/cm^2)	8.64	6.64	7.23	6.32	5.66	0.60	0.70	0.72	0.73	0.77
Chl *a* (μg/cm^2)	5.97	4.75	5.25	4.65	4.15	0.63	0.72	0.72	0.73	0.78
Chl *b* (μg/cm^2)	2.73	1.92	2.06	1.89	1.69	0.48	0.67	0.69	0.69	0.73
Car (μg/cm^2)	1.71	1.31	1.29	1.22	1.12	0.48	0.65	0.69	0.69	0.73
N_{mass} (%)	1.62	0.42	0.51	0.37	0.29	0.08	0.36	0.07	0.36	0.62
C_{mass} (%)	1.59	1.71	1.74	1.26	1.03	0.20	0.21	0.19	0.39	0.56
LMA (g/cm^2)	61.13	27.17	24.86	21.78	18.76	0.13	0.71	0.75	0.79	0.85

Table 5
Performance of PLSR reflectance models that were calibrated using data from one site and validated using data from the other site.

Leaf traits	RMSE		R^2	
	MV → HF	HF → MV	MV → HF	HF → MV
Total Chl (μg/cm^2)	6.17	7.44	0.72	0.67
Chl *a* (μg/cm^2)	4.39	5.29	0.73	0.69
Chl *b* (μg/cm^2)	1.85	1.99	0.68	0.66
Car (μg/cm^2)	1.19	1.54	0.59	0.59
N_{mass} (%)	0.56	0.72	0.29	0.20
C_{mass} (%)	2.89	2.90	0.10	0.23
LMA (g/cm^2)	35.62	59.45	0.60	0.72

well, indicating both sites share similar wavelength regions (Fig. S11). As a result, cross-site prediction of leaf pigments showed reasonable accuracy (Table 5). It also has important implications for the design of multiband sensors and imagers as it can select the wavelengths that are most useful for the leaf traits of interest (Nijland et al., 2014; Ryu et al., 2010).

The variability of our seven leaf traits was not equally captured (Table 3). The absorption features of pigments are well understood and clearly represented in the VIP value plots (Fig. 6). While for C_{mass} and N_{mass}, although there have been studies on the possible linkage between certain components in the leaves (e.g., protein, cellulose) and leaves' optical properties, the impact on leaf spectra is is less pronounced in any single spectral range as compared with pigments and instead is more generally spread across the visible and shortwave infrared spectral regions (Curran, 1989; Kokaly et al., 2009). This may partly explain the less accurate PLSR models for the C_{mass} and N_{mass}. Moreover, in fresh leaves the spectral absorption by proteins can be partially obscured by water absorption, which can impact the performance of statistical (e.g. PLSR, SVIs) and other spectral inversion approaches, such as radiative transfer models (RTMs).

As expected, the PLSR approach, which can exploit the full spectrum information to estimate leaf traits performed better than traditional SVIs (Table 3). While SVIs that were calibrated with extensive datasets displayed a similar performance to PLSR in estimating total chlorophyll concentration, we observed better performance of PLSR for the carotenoids and LMA. Calibrating SVIs with our own datasets did not improve their performance. In addition, we calculated the correlation coefficient (r) of all possible two-band SVIs with total chlorophyll, carotenoids, and LMA (Fig. S13). We found that the highest correlation (in terms of the absolute value of r) between the SVIs and three leaf traits are −0.8, −0.7, and −0.65, respectively. This suggests that the variability of leaf traits in our dataset was not fully captured by the SVIs, despite that our dataset covering a broad ranges of values observed by others (Féret et al., 2011). Incorporating more datasets to the calibration of simple indices could potentially improve the performance of these methods, but will not alleviate the saturation issue that is pervasive when using simple SVIs, especially for LMA.

As the applications of leaf spectra-traits relationship become more common, we argue that a standardized protocol to calibrate and validate PLSR-type models is needed. This includes independent validation to avoid evaluating model performance against the calibration dataset itself and a method to choose the optimal number of PLSR components to prevent overfitting (Serbin et al., 2014; Wu et al., 2016b). A globally relevant algorithm for leaf traits that can be used by ground spectral observations (Hilker, Nesic, Coops, & Lessard, 2010), upcoming (e.g., EnMAP; Guanter et al., 2015) or existing or planned satellite missions such as NASA's HyspIRI mission (such as https://hyspiri.jpl.nasa.gov/; Lee et al., 2015) hinges on a rigorously-tested method and on datasets covering a wide range of variations in leaf traits.

4.2. The implications for field sampling strategy

The time-series of leaf traits we presented here showed the critical time windows to capture trait seasonality. These patterns are similar to observations on other temperate species (e.g. McKown et al. (2013)). Extensive field sampling is laborious and expensive and the continual question in plant ecology is "how much is good enough?" Since the measurements of leaf spectral properties are less labor-intensive (and non-destructive) compared with the measurements of most leaf traits, we explored how many destructive measurements of leaf traits were needed to calibrate the models using full leaf spectra. For example, LMA showed dramatic changes in the early season, thus the sampling and calibration process needs to include the data at this critical phenophase (Fig. 2a). Similarly, N_{mass} was relatively stable in the mid season, and most of the variations occurred in the beginning and end of season, which makes the sampling at these time points important (Fig. 2b). This explains why our comparisons that only considered the variability of leaf traits in the summer showed poorer performance, as compared to a model capturing the full seasonal variability Therefore, monthly and even biweekly sampling should be considered, at least for the four temperate deciduous species examined in this study.

4.3. Broad implications of using leaf spectroscopy for ecological studies

Understanding the seasonality of leaf traits has recently gained attention as an effort to improve our modeling of terrestrial carbon and water cycles (Bauerle et al., 2012; Grassi, Vicinelli, Ponti, Cantoni, & Magnani, 2005; Medvigy, Jeong, Clark, Skowronski, & Schäfer, 2013). For example, in the Community Land Model, N_{mass} and LMA control the maximum rate of carboxylation, V_{cmax}, which is highly variable temporally and across different species and light environments (Oleson, Lawrence, Bonan, et al., 2013). Our time-series of N_{mass} capture two important features: (1) the seasonal peak at the beginning of the spring, suggesting that nitrogen was allocated to the leaves early in the season. As leaves matured, other types of elements such as carbon accumulated at a faster rate, resulting in an increase of C_{mass} relative to N_{mass} ratio. (2) A decline of N_{mass} by the end of the season. N_{mass} and LMA was relatively stable at both sites during the summer (Fig. 2a and b), thus leaf age does not appear to be affecting the nitrogen concentration during the peak season (Field & Mooney, 1983). This finding as that of others (McKown et al., 2013; Wilson et al., 2000) highlights the importance of tracking the seasonality of leaf traits, and our work demonstrates that leaf spectroscopy can provide a rapid means to routinely measure leaf traits. Importantly, these results highlight that spectroscopy observations can provide key information on the individual differences in multiple leaf traits that can feed into ecosystem models (Medvigy, Wofsy, Munger, Hollinger, & Moorcroft, 2009) or be used to test key ecological hypotheses (Rowland et al., 2015). Our results suggest the important capability of monitoring ecosystem dynamics across a range of spatial and temporal scales with hyperspectral observations from leaves, towers, as well as with new instruments mounted on unmanned and piloted aircraft and satellite platforms (Asner & Martin, 2008; Hilker et al., 2010; Yang et al., 2014; Yang et al., 2015).

5. Conclusion

This paper presents a comprehensive study of the relationship between leaf spectra and foliar traits across varying leaf developmental stages, sites, and light environment using a near weekly dataset of seven leaf traits and spectra at two sites. A Partial Least Square Regression (PLSR) modeling approach, after proper calibration with leaf traits from different times of the season, showed a strong capacity to quantify the seasonal variation of leaf traits within and across sites. The robustness of a PLSR model largely depends on the overlap of leaf trait ranges between the calibration dataset and the dataset to be estimated, and extrapolation outside the ranges of the calibration dataset can result in a significant error. We found that biweekly sampling of leaf traits and spectra would provide a robust PLSR model to estimate the seasonal variations of leaf traits. This work demonstrated the capability of leaf

spectra to track seasonally varying leaf traits, and thus supports the use of automated field spectrometers, airborne and satellite hyperspectral sensors to track leaf traits repeatedly throughout the season and across broad regions (Roberts, Quattrochi, Hulley, Hook, & Green, 2012; Singh, Serbin, McNeil, Kingdon, & Townsend, 2015; Yang et al., 2015).

Acknowledgements

We thank Katie Laushman, Lakiah Clark, Skyler Hackley, Rui Zhang, Kate Morkeski, Mengdi Cui, Marc Mayes and Tim Savas for assisting with fieldwork. We thank Matthew Erickson, Marshall Otter, Rich McHorney, Jane Tucker and Sam Kelsey from the Marine Biological Laboratory for the help with labwork. We also thank the Harvard Forest, the Manuel F. Correllus State Forest, Nature's Conservancy Hoft Farm Preserve and Mr. Colbert for the permission to use the forests for research. This research was supported by the Brown University—Marine Biological Laboratory graduate program in Biological and Environmental Sciences, and Marine Biological Laboratory start-up funding for JT. JT was also partially supported by the U.S. Department of Energy (DOE) Office of Biological and Environmental Research grant DE-SC0006951 and the National Science Foundation grants DBI-959333 and AGS-1005663. SPS was supported in part by the U.S. DOE contract No. DE-SC00112704 to Brookhaven National Laboratory. JW was supported by the NASA Earth and Space Science Fellowship (NESSF2014).

Appendix A. Supplementary data

Supplementary data to this article can be found online at http://dx.doi.org/10.1016/j.rse.2016.03.026.

References

Asner, G., & Martin, R. (2008). Spectral and chemical analysis of tropical forests: Scaling from leaf to canopy levels. *Remote Sensing of Environment*, *112*, 3958–3970.

Asner, G. P., & Vitousek, P. M. (2005). Remote analysis of biological invasion and biogeochemical change. *Proceedings of the National Academy of Sciences of the United States of America*, *102*, 4383–4386.

Asner, G. P., Martin, R. E., Ford, A., Metcalfe, D., & Liddell, M. (2009). Leaf chemical and spectral diversity in Australian tropical forests. *Ecological Applications*, *19*, 236–253.

Bauerle, W. L., Oren, R., Way, D. A., Qian, S. S., Stoy, P. C., Thornton, P. E., ... Reynolds, R. F. (2012). Photoperiodic regulation of the seasonal pattern of photosynthetic capacity and the implications for carbon cycling. *Proceedings of the National Academy of Sciences*, *109*, 8612–8617.

Belanger, M., Miller, J., & Boyer, M. (1995). Comparative relationships between some red edge parameters and seasonal leaf chlorophyll concentrations. *Canadian Journal of Remote Sensing*, *21*, 16–21.

Bonan, G. B., Oleson, K. W., Fisher, R. A., Lasslop, G., & Reichstein, M. (2012). Reconciling leaf physiological traits and canopy flux data: Use of the TRY and FLUXNET databases in the Community Land Model version 4. *Journal of Geophysical Research: Biogeosciences*, *117*, G02026.

Couture, J. J., Serbin, S. P., & Townsend, P. A. (2013). Spectroscopic sensitivity of real-time, rapidly induced phytochemical change in response to damage. *New Phytologist*, *198*, 311–319.

Curran, P. J. (1989). Remote sensing of foliar chemistry. *Remote Sensing of Environment*, *30*, 271–278.

Demmig-Adams, B., & Adams, W. W. (2000). Photosynthesis: Harvesting sunlight safely. *Nature*, *403*, 371–374.

Dillen, S. Y., de Beeck, M. O., Hufkens, K., Buonanduci, M., & Phillips, N. G. (2012). Seasonal patterns of foliar reflectance in relation to photosynthetic capacity and color index in two co-occurring tree species, *Quercus rubra* and *Betula papyrifera*. *Agricultural and Forest Meteorology*, *160*, 60–68.

Eckstein, R. L., Karlsson, P. S., & Weih, M. (1999). Leaf life span and nutrient resorption as determinants of plant nutrient conservation in temperate-arctic regions. *New Phytologist*, *143*, 177–189.

Ellsworth, D. S., & Reich, P. B. (1993). Canopy structure and vertical patterns of photosynthesis and related leaf traits in a deciduous forest. *Oecologia*, *96*, 169–178.

Evans, J. (1989a). Photosynthesis and nitrogen relationships in leaves of C3 plants. *Oecologia*, *78*, 9–19.

Evans, J. (1989b). Partitioning of nitrogen between and within leaves grown under different irradiances. *Australian Journal of Plant Physiology*, *16*(6), 533–548.

Féret, J. -B., François, C., Gitelson, A., Asner, G. P., Barry, K. M., Panigada, C., ... Jacquemoud, S. (2011). Optimizing spectral indices and chemometric analysis of leaf chemical properties using radiative transfer modeling. *Remote Sensing of Environment*, *115*, 2742–2750.

Field, C., & Mooney, H. A. (1983). Leaf age and seasonal effects on light, water, and nitrogen use efficiency in a California shrub. *Oecologia*, *56*, 348–355.

Fisher, J., & Mustard, J. (2007). Cross-scalar satellite phenology from ground, Landsat, and MODIS data. *Remote Sensing of Environment*, *109*, 261–273.

Foster, D., Hall, B., Barry, S., Clayden, S., & Parshall, T. (2002). Cultural, environmental and historical controls of vegetation patterns and the modern conservation setting on the island of Martha's Vineyard, USA. *Journal of Biogeography*, *29*, 1381–1400.

Garrity, S. R., Vierling, L. A., & Bickford, K. (2010). A simple filtered photodiode instrument for continuous measurement of narrowband NDVI and PRI over vegetated canopies. *Agricultural and Forest Meteorology*, *150*, 489–496.

Grassi, G., Vicinelli, E., Ponti, F., Cantoni, L., & Magnani, F. (2005). Seasonal and interannual variability of photosynthetic capacity in relation to leaf nitrogen in a deciduous forest plantation in northern Italy. *Tree Physiology*, *25*, 349–360.

Guanter, L., Kaufmann, H., Segl, K., Foerster, S., Rogass, C., Chabrillat, S., Kuester, T., Hollstein, A., Rossner, G., & Chlebek, C. (2015). The EnMAP spaceborne imaging spectroscopy mission for earth observation. *Remote Sensing*, *7*, 8830–8857.

Hilker, T., Coops, N. C., Coggins, S. B., Wulder, M. A., Brownc, M., Black, T. A., ... Lessard, D. (2009). Detection of foliage conditions and disturbance from multi-angular high spectral resolution remote sensing. *Remote Sensing of Environment*, *113*, 421–434.

Hilker, T., Nesic, Z., Coops, N. C., & Lessard, D. (2010). A new, automated, multiangular radiometer instrument for tower-based observations of canopy reflectance (Amspec Ii). *Instrumentation Science & Technology*, *38*, 319–340.

Huete, A., Didan, K., Miura, T., Rodriguez, E. P., Gao, X., & Ferreira, L. G. (2002). Overview of the radiometric and biophysical performance of the MODIS vegetation indices. *Remote Sensing of Environment*, *83*, 195–213.

Jacquemoud, S., & Baret, F. (1990). PROSPECT: A model of leaf optical properties spectra. *Remote Sensing of Environment*, *34*, 75–91.

Kattge, J., Díaz, S., Lavorel, S., Prentice, I. C., Leadley, P., Bönisch, G., ... Wirth, C. (2011). TRY — A global database of plant traits. *Global Change Biology*, *17*, 2905–2935.

Kennard, R. W., & Stone, L. A. (1969). Computer aided design of experiments. *Technometrics*, *11*, 137–148.

Kokaly, R. F., Asner, G. P., Ollinger, S. V., Martin, M. E., & Wessman, C. A. (2009). Characterizing canopy biochemistry from imaging spectroscopy and its application to ecosystem studies. *Remote Sensing of Environment*, *113*, S78–S91.

Laisk, A., Nedbal, L., & Govindjee (2009). *Photosynthesis in silico: Understanding complexity from molecules to ecosystems.* Springer Science & Business Media.

Lee, C. M., Cable, M. L., Hook, S. J., Green, R. O., Ustin, S. L., Mandl, D. J., & Middleton, E. M. (2015). An introduction to the NASA Hyperspectral InfraRed Imager (HysplRI) mission and preparatory activities. *Remote Sensing of Environment*, *167*, 6–19.

Lewandowska, M., & Jarvis, P. (1977). Changes in chlorophyll and carotenoid content, specific leaf area and dry weight fraction in Sitka spruce, in response to shading and season. *New Phytologist*, *79*, 247–256.

Lichtenthaler, H. K., & Buschmann, C. (2001). Chlorophylls and carotenoids: Measurement and characterization by UV–VIS spectroscopy. *Current protocols in food analytical chemistry*. John Wiley & Sons, Inc.

McKown, A. D., Guy, R. D., Azam, M. S., Drewes, E. C., & Quamme, L. K. (2013). Seasonality and phenology alter functional leaf traits. *Oecologia*, *172*, 653–665.

Medvigy, D., Jeong, S. -J., Clark, K. L., Skowronski, N. S., & Schäfer, K. V. R. (2013). Effects of seasonal variation of photosynthetic capacity on the carbon fluxes of a temperate deciduous forest. *Journal of Geophysical Research: Biogeosciences*, *118*, 1703–1714.

Medvigy, D., Wofsy, S. C., Munger, J. W., Hollinger, D. Y., & Moorcroft, P. R. (2009). Mechanistic scaling of ecosystem function and dynamics in space and time: Ecosystem demography model version 2. *Journal of Geophysical Research: Biogeosciences*, *114*, G01002. http://dx.doi.org/10.1029/2008JG000812.

Mehmood, T., Liland, K. H., Snipen, L., & Sæbø, S. (2012). A review of variable selection methods in partial least squares regression. *Chemometrics and Intelligent Laboratory Systems*, *118*, 62–69.

Niinemets, U. (2007). Photosynthesis and resource distribution through plant canopies. *Plant Cell and Environment*, *30*(9), 1052–1071.

Nijland, W., de Jong, R., de Jong, S. M., Wulder, M. A., Bater, C. W., & Coops, N. C. (2014). Monitoring plant condition and phenology using infrared sensitive consumer grade digital cameras. *Agricultural and Forest Meteorology*, *184*, 98–106.

Oleson, K. W., Lawrence, D. M., Bonan, G. B., Flanner, M. G., Kluzek, E., Lawrence, P. J., ... Zeng, X. (2013). *Technical Description of version 4.5 of the Community Land Model (CLM). Ncar Technical Note NCAR/TN-503 + STR.* National Center for Atmospheric Research, Boulder, CO,. http://dx.doi.org/10.5065/D6RR1W7M.

Poorter, H., Niinemets, Ü., Poorter, L., Wright, I. J., & Villar, R. (2009). Causes and consequences of variation in leaf mass per area (LMA): A meta-analysis. *New Phytologist*, *182*, 565–588.

Richardson, A. D., Duigan, S. P., & Berlyn, G. P. (2002). An evaluation of noninvasive methods to estimate foliar chlorophyll content. *New Phytologist*, *153*, 185–194.

Roberts, D. A., Quattrochi, D. A., Hulley, G. C., Hook, S. J., & Green, R. O. (2012). Synergies between VSWIR and TIR data for the urban environment: An evaluation of the potential for the Hyperspectral Infrared Imager (HysplRI) Decadal Survey mission. *Remote Sensing of Environment*, *117*, 83–101.

Rowland, L., da Costa, A. C. L., Galbraith, D. R., Oliveira, R. S., Binks, O. J., Oliveira, A. A. R., ... Meir, P. (2015). Death from drought in tropical forests is triggered by hydraulics not carbon starvation. *Nature*, *528*(7580), 119–122. http://dx.doi.org/10.1038/nature15539.

Ryu, Y., Baldocchi, D. D., Verfaillie, J., Ma, S., Falk, M., Ruiz-Mercado, I., ... Sonnentag, O. (2010). Testing the performance of a novel spectral reflectance sensor, built with light emitting diodes (LEDs), to monitor ecosystem metabolism, structure and function. *Agricultural and Forest Meteorology*, *150*, 1597–1606.

Schimel, D., Pavlick, R., Fisher, J. B., Asner, G. P., Saatchi, S., Townsend, P., ... Cox, P. (2015). Observing terrestrial ecosystems and the carbon cycle from space. *Global Change Biology*, *21*, 1762–1776.

Schneider, C. A., Rasband, W. S., & Eliceiri, K. W. (2012). NIH image to ImageJ: 25 years of image analysis. *Nature Methods*, *9*, 671–675.

Serbin, S. P., Singh, A., McNeil, B. E., Kingdon, C. C., & Townsend, P. A. (2014). Spectroscopic determination of leaf morphological and biochemical traits for northern temperate and boreal tree species. *Ecological Applications*, *24*, 1651–1669.

Shen, M., Chen, J., Zhu, X., & Tang, Y. (2009). Yellow flowers can decrease NDVI and EVI values: Evidence from a field experiment in an alpine meadow. *Canadian Journal of Remote Sensing*, *35*, 99–106.

Sims, D. A., & Gamon, J. A. (2002). Relationships between leaf pigment content and spectral reflectance across a wide range of species, leaf structures and developmental stages. *Remote Sensing of Environment*, *81*, 337–354.

Singh, A., Serbin, S. P., McNeil, B. E., Kingdon, C. C., & Townsend, P. A. (2015). Imaging spectroscopy algorithms for mapping canopy foliar chemical and morphological traits and their uncertainties. *Ecological Applications*.

Terashima, I., Miyazawa, S. -I., & Hanba, Y. T. (2001). Why are sun leaves thicker than shade leaves?—Consideration based on analyses of CO_2 diffusion in the leaf. *Journal of Plant Research*, *114*, 93–105.

Ustin, S. L., Gitelson, A. A., Jacquemoud, S., Schaepman, M., Asner, G. P., Gamon, J. A., & Zarco-Tejada, P. (2009). Retrieval of foliar information about plant pigment systems from high resolution spectroscopy. *Remote Sensing of Environment*, *113*, S67–S77.

Ustin, S. L., Roberts, D. A., Gamon, J. A., Asner, G. P., & Green, R. O. (2004). Using imaging spectroscopy to study ecosystem processes and properties. *Bioscience*, *54*, 523–534.

Wicklein, H. F., Ollinger, S. V., Martin, M. E., Hollinger, D. Y., Lepine, L. C., Day, M. C., ... Norby, R. J. (2012). Variation in foliar nitrogen and albedo in response to nitrogen fertilization and elevated CO2. *Oecologia*, *169*, 915–925.

Wilson, K. B., Baldocchi, D. D., & Hanson, P. J. (2000). Spatial and seasonal variability of photosynthetic parameters and their relationship to leaf nitrogen in a deciduous forest. *Tree Physiology*, *20*, 565–578.

Wofsy, S. C., Goulden, M. L., Munger, J. W., Fan, S. -M., Bakwin, P. S., Daube, B. C., ... Bazzaz, F. A. (1993). Net Exchange of CO_2 in a Mid-Latitude Forest. *Science*, *260*, 1314–1317.

Wold, S., Sjöström, M., & Eriksson, L. (2001). PLS-regression: A basic tool of chemometrics. *Chemometrics and Intelligent Laboratory Systems*, *58*, 109–130.

Wright, I. J., Reich, P. B., Westoby, M., Ackerly, D. D., Baruch, Z., Bongers, F., ... Villar, R. (2004). The worldwide leaf economics spectrum. *Nature*, *428*, 821–827.

Wu, J., Albert, L. P., Lopes, A. P., Restrepo-Coupe, N., Hayek, M., Wiedemann, K. T., Guan, K., Stark, S. C., et al. (2016a). Leaf development and demography explain photosynthetic seasonality in Amazon evergreen forests. *Science*, *351*, 972–976.

Wu, J., Chavana-Bryant, C., Prohaska, N., Serbin, S. P., Guan, K., Albert, L. P., ... Saleska, S. (2016b). *Convergence in relations among leaf traits, spectra and ages across diverse canopy environments and two contrasting tropical forests.* New Phytologist Accepted.

Yang, X., Mustard, J., Tang, J., & Xu, H. (2012). Regional-scale phenology modeling based on meteorological records and remote sensing observations. *Journal of Geophysical Research*, *117*, G03029.

Yang, X., Tang, J., & Mustard, J. (2014). Beyond leaf color: Comparing camera-based phenological metrics with leaf biochemical, biophysical and spectral properties throughout the growing season of a temperate deciduous forest. *Journal of Geophysical Research: Biogeosciences*, *119*, 181–191.

Yang, X., Tang, J., Mustard, J. F., Lee, J. -E., Rossini, M., Joiner, J., ... Richardson, A. D. (2015). Solar-induced chlorophyll fluorescence that correlates with canopy photosynthesis on diurnal and seasonal scales in a temperate deciduous forest. *Geophysical Research Letters*, *42*, 2977–2987.

Zhang, Y., Chen, J. M., & Thomas, S. C. (2007). Retrieving seasonal variation in chlorophyll content of overstory and understory sugar maple leaves from leaf-level hyperspectral data. *Canadian Journal of Remote Sensing*, *33*, 406–415.

Zhao, K., Valle, D., Popescu, S., Zhang, X., & Mallick, B. (2013). Hyperspectral remote sensing of plant biochemistry using Bayesian model averaging with variable and band selection. *Remote Sensing of Environment*, *132*, 102–119.